processes

MDPI

Article

Numerical Investigation of the Use of Boron Nitride/Water and Conventional Nanofluids in a Microchannel Heat Sink

Fuat Kaya

Department of Mechanical Engineering, Nigde Omer Halisdemir University, Nigde 51240, Turkey; fkaya@ohu.edu.tr; Tel.: +90-388-2252480; Fax: +90-388-2250112

Abstract: The purpose of this paper is to study the effects of the use of boron nitride (BN) and other conventional nanoparticles (Al_2O_3, CuO and TiO_2) on pressure drop and heat transfer in a microchannel. The governing equations for forced fluid flow and heat transfer were worked out by using fluent computational fluid dynamics (CFD) code. Computational results collected from fluent CFD code for Al_2O_3 as the nano-particle were compared with numerical values used in the literature for validation. The basis of a water-cooled (pure water, Al_2O_3/Water, CuO/Water, TiO_2/Water and BN/Water) smooth microchannel was outlined, and then the corresponding laminar flow and heat transfer were evaluated numerically. The results from the numerical tests (NT) express good agreement with the values found in the literature. These results also indicate, through the comparison which was performed by taking the heat transfer and pressure loss parameters between BN and other widely used conventional nanoparticles (Al_2O_3, CuO and TiO_2) into consideration, that BN is the more favorable nanoparticle. In comparison to other common nanoparticles (Al_2O_3, CuO and TiO_2), BN enhances heat transfer and slightly raised pressure losses owing to its high thermal conductivity and high velocity profile because of low density. It is also chemically stable at the highest temperature relative to most solid materials. Thus, it has a structure that can be used in cooling systems for a long time without causing a problem of agglomeration.

Keywords: microchannel; nanofluid; CFD; pressure drop; heat transfer; boron nitride

Citation: Kaya, F. Numerical Investigation of the Use of Boron Nitride/Water and Conventional Nanofluids in a Microchannel Heat Sink. *Processes* **2022**, *10*, 2639. https://doi.org/10.3390/pr10122639

Academic Editors: Rui A. Lima and Titan C. Paul

Received: 18 November 2022
Accepted: 4 December 2022
Published: 8 December 2022

1. Introduction

The high-power density and compactness characteristic of modern electronic devices require the use of efficient and compact cooling components for these devices. The primary task of these components is to maintain this high power and therefore heat generating electronics packages within their designed operating temperature range [1,2]. To ensure the reliability of electronics, many heat dissipation methods have been suggested, which include microchannel heat sink, jet impingement, heat pipe, and thin film boiling, etc. In contrast to conventional heat sinks, which require a large surface area to increase heat dissipation rates, microchannel heat sinks seem applicable for this purpose since they are small and effective.

A microchannel heat sink comprises small diameter passages for a liquid coolant. Creating a large area for the heat transfer between the cooler and the device to be cooled is achieved using these small diameter passages.

Microchannels are fluid flow channels with small hydraulic diameters. Following the classification by Kandlikar and Grande [3], channels with a minimum cross-sectional dimension between 200 µm and 3 mm are classified as minichannels and those between 1 µm and 200 µm are classified as microchannels. The flow in microchannels has been the subject of increased research interest over the past few years. It can be seen in many important applications, such as miniature heat exchangers, microscale process units, nuclear reactors, material processing and thin film deposition technology, and biotechnology system, as well as potentially in space applications [4]. A great deal of research has

been carried out to improve the thermal performance of micro systems, according to the literature [5–9].

Zunaid et al. [10] studied the heat transfer and pressure drop characteristics of a straight, rectangular and semi-cylindrical projection microchannel heat sink. They stated that heat transfer increases with the use of semi-cylindrical projection microchannel heat sink.

It is difficult to cool a heated system with traditional liquids, owing to the high-power and high-integration demand, so researchers have concentrated on nanofluids.

A nanofluid is a fluid containing nanometer-sized particles [11]. These particles are metals or metal-oxides [12]. Water is used as the main fluid in nanofluids due to its thermal performance properties.

Abdolahi et al. [13] investigated the fluid flow and heat transfer characteristics of laminar nanofluid flow in microchannel heat sink (MCHS) with V-Type inlet/outlet arrangement, and showed that nanofluid can improve the performance of MCHS with V-shaped inlet/outlet arrangement.

Coskun and Cetkin [14] showed that overall thermal conductance in a rectangular microchannel heat sink can be maximized with the combination of nanofluids and micro pin fins. They showed the effect of micro pin fins and nanofluids both separately and simultaneously, in order to show their effect on the thermal conductance (i.e., thermal resistance). Both nanofluids and micro pin fins decrease the overall thermal resistance due to the increase in the average thermal conductivity of the flow system.

Sabaghan et al. [15] researched a comprehensive numerical procedure which is based on the two-phase approach to simulate a rectangular microchannel consisting of six longitudinal vortex generators (LVGs), and stated that using the mixture of EG:W (60:40 ethylene glycol and water) instead of pure water as a base-fluid leads to the increase of heat transfer in the microchannel. Finally, the maximum normalized efficiency of the LVG-enhanced microchannel, compared to the plain channel, is around 14%. Furthermore, using nanofluid can improve the normalized efficiency by 27%.

Belhadj et al. [16] used a numerical study to show that laminar forced the convective flow of nanofluid-based water/Al_2O_3 in a two-dimensional horizontal microchannel heat sink. They stated that their study contributes to improving cooling systems by integrating the nanofluids in the next generation of microchannel heat sinks.

Shi et al. [17] created a new simulation method, which is described in their paper, to consider whether the thermophysical properties of nanofluids are non-uniform and dynamic in the channels. It was validated by the classical experimental data. The effects of the concentration of nanoparticles, the Reynolds number and the axial thermal conduction effect on the flow and heat transfer characteristics of nanofluids in microchannels are analyzed. They concluded that the proposed numerical simulation method can simulate the forced flow and heat transfer of nanofluids in the microchannel more accurately than the traditional single-phase model.

A numerical study was performed by Kahani [18] to investigate the heat performance of Al_2O_3/water as a nanofluid in a microchannel. He used a modified dispersion model to take the effect of the nanoparticle into account, and recommended this model to predict the thermal performance effects well. Moreover, he stated that the best thermal performance is obtained at a 0.526 aspect ratio of the microchannel.

Gonçalves et al. [19] studied forced convective heat transfer by using different geometrical parameters of a microchannel in a single-phase flow of the fluid. They stated that the higher heat performance of the microchannel comprised a rectangular collector with eight microchannels and vertical placement of the inlet and outlet.

Zainon et al. [20] studied the thermo-physical properties of TiO_2-SiO_2 hybrid nanofluids at volume concentrations between 0.5 and 1.5%. They stated that the thermophysical properties of TiO_2-SiO_2 hybrid nanofluids are temperature-dependent. Both thermal conductivity and specific heat are seen to increase with temperature. In contrast, the viscosity and density decreased when the temperature increase. Based on these findings, the TiO_2-

SiO_2 hybrid nanofluids at the recommended volume concentration of 1.5% can be used to replace conventional heat transfer fluids.

Researchers have made great efforts to improve thermal performance in cooling systems by developing or using different nanofluids in different methods.

Saba et al. [21] investigated the three-dimensional compression flow of the hybrid nanofluid (CNT-SiO_2/H_2O). They used an improved Hamilton-Crosser model (RHCM) to explain the effective thermal conductivity of nanofluid based on CNTs. Expressions for the local Nusselt number and skin friction coefficient were also obtained, and their effective behavior was briefly discussed.

Researchers are daily proposing new nanofluids as an alternative to traditional nanofluids.

Rashid et al. [22] investigated the shape effects of graphene-water nanofluid flow on the Marangoni boundary layer and heat transfer over a porous medium under the effects of the suction parameter. They compared the thermal performance by suspending nanoparticles in various shapes.

Studies on the effects of boron minerals as nanofluids are very limited in quantity in the literature, in spite of the fact that these minerals are significant for cooling systems. Furthermore, the presence of new nanofluids helps considerably in solving the problems of cooling systems.

Han et al. [23] created boron nitride nanospheres without requiring modification or the addition of surfactants. Thus, they expressed that BN nanospheres have great potential for improving the thermal conductivity of water-based fluids.

Hou et al. [24] showed a new nanofluid called boron nitride nanosheets with regard to its thermal performance.

Velmurugan et al. [25] studied the effect of boron nitride as nanoparticle. They recommended it as a nanoparticle in nanofluid systems because, due to its high thermal conductivity, appropriate thermal expansion coefficient, high electrical insulation and high mechanical strength, it is a promising addition to traditional heat exchange fluids.

Boron nitride is a ceramic material that has been studied as a nanoparticle due to its high thermal performance properties. In addition, it is also chemically stable with respect to most solid materials, even at most high temperatures. Recently, these particles have become the focus of attention of researchers and industry due to their superior properties.

Kumar and Tiwari [26] evaluated the thermal performance of a U-tube evacuated tube solar collector using water-based and different concentrations of boron nitride. They analyzed the thermal performance of the collector at different mass flow rates and obtained approximately maximum energy efficiency (72.14% at 1.5% volume and 0.051 kg/s). This corresponds to 84% higher efficiency than pure water fluid under the same flow conditions.

Zu et al. [27] studied the application of TiN-modified h-BN nanolayers in solar collectors. They stated that their work is important for new strategies to use the full spectrum of solar energy and to control the photothermal properties of nanofluids.

Mat et al. [28] reported the results of a numerical simulation by CFD on the liquid flow of Triton TX-100 surfactant containing boron nitride nanotubes (BNN) in distilled water (base liquid) at 30 and 50 °C.

Due to the rapid advances in cooling systems and the high thermal performance requirement in these systems, intensive studies are carried out on nanofluids. These studies are about obtaining new and high-performance nanofluids as an alternative to existing nanofluids. In this context, nano-sized solid particles used in nanofluid content should have superior properties in terms of heat transfer and pressure drop. Recently, studies on obtaining nanofluids using BN nanoparticles and using them in cooling systems have increased due to their high thermal capacity, stability at high temperatures and low-density properties.

For this reason, in this study, to acquire the effect of the use of boron nitride (BN) and other conventional nanoparticles (Al_2O_3, CuO and TiO_2) in a microchannel on pressure drop and heat transfer, the 3-D numerical simulations by using the fluent CFD code were evaluated. The geometrical dimensions studied in this paper are demonstrated in

Shi et al. [17]. Boron nitride (BN) and other conventional nanoparticles (Al_2O_3, CuO and TiO_2) are used with water as a base fluid by changing the inlet Reynolds number and the volume fraction ratio. It was calculated which of these four nanoparticles have better properties in terms of pressure drop and heat transfer characteristics.

2. Materials and Methods

2.1. Governing and Additional Equations

Governing equations for incompressible, steady state, laminar flow and heat transfer in a microchannel were calculated numerically using fluent CFD code.

The steady-state conservation of mass, momentum and energy equations can be shown in the following compact form:

$$\nabla\cdot(\rho\vec{U}) = 0 \tag{1}$$

$$\nabla(\rho\vec{U}\vec{U}) = -\nabla P + \nabla\cdot(\mu\nabla\vec{U}) + S_m \tag{2}$$

$$\nabla(\rho\vec{U}c_pT) = -\nabla\cdot(k\nabla T) + S_e \tag{3}$$

where S_m and S_e are the source terms and represent the momentum and energy transfer between the continuous phase and the discrete phase, respectively [17].

$$S_m = \sum n_p \frac{m_p}{\delta U}\frac{dU_p}{dt} \tag{4}$$

$$S_e = \sum n_p \frac{m_p}{\delta U}C_p\frac{dT_p}{dt} \tag{5}$$

n_p is the number of nanoparticles in a computational cell.

$$\frac{dU_p}{dt_p} = \frac{18\mu_c}{\rho_p d_p^2}\frac{C_D\mathrm{Re}_p}{24}(U_c - U_p) + \frac{g(\rho_p - \rho_c)}{\rho_c} + F_{other} \tag{6}$$

where C_D is the drag coefficient.

$$C_D = \frac{24}{\mathrm{Re}_p} \tag{7}$$

The relative Reynolds number of nanoparticles Re_p is

$$\mathrm{Re}_p = \frac{\rho d_p|u - u_p|}{\mu} \tag{8}$$

Moving nanoparticles from the high temperature region to the low temperature region:

$$F_{tp} = -3\pi\mu^2 d_p K_{tp}\frac{\nabla T}{\rho_f T} \tag{9}$$

where K_{tp} is a function of the thermal conductivities of both the fluid and the solid particle [29].

The force resulting from the collisions between the particles and randomly moving molecules of the base fluid leads to the Brownian motion of the nanoparticles.

$$F_{Br} = \frac{m_p}{\pi}\vec{R}\sqrt{\frac{2k_BT}{3\pi\mu d_p(\Delta t)^3}} \tag{10}$$

where R is a random vector and Δt is the integration time [29].

Heat transfer coefficient h is calculated using the Ranz and Marshall correction [30].

$$Nu = \frac{h\cdot d_p}{k} = 2 + 0.6\cdot\mathrm{Re}_p^{1/2}\cdot\mathrm{Pr}^{1/3} \tag{11}$$

where Pr is the Prandtl number.

For the simulations, a uniform heat flux of 200,000 W/cm^2 was applied on the bottom surface of the substrate. The top wall surface of the channels and the outer surfaces of the microchannel were assumed to be insulated. For the flow field, the velocity applied at the inlet was assumed to be uniform and a pressure condition was applied at the outlet. Thermal radiation and natural convection heat transfer between the outer wall surface and the environment were ignored.

2.2. Numerical Procedure

The microchannel used in the numerical tests had an overall length of 44.8 mm and the hydraulic diameter of 341 µm, as can be seen in Figure 1.

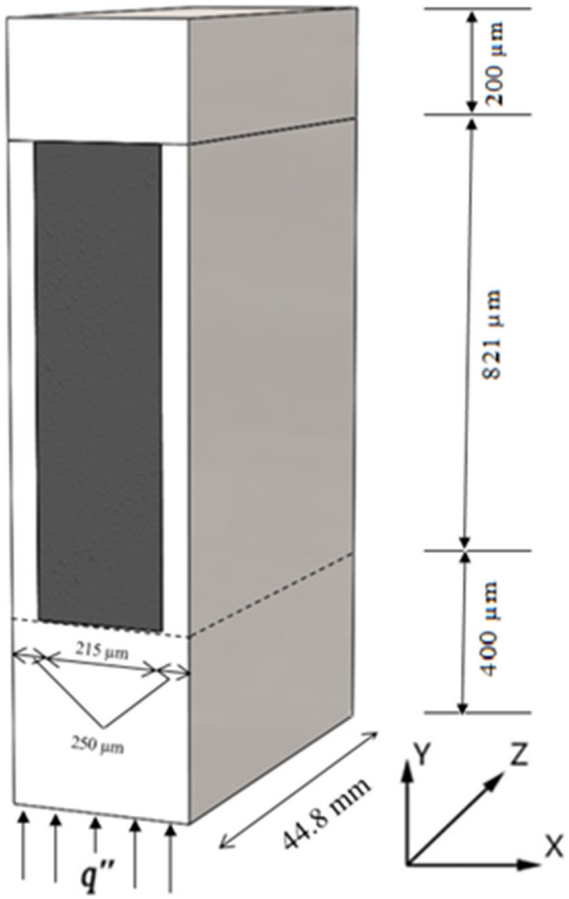

Figure 1. Dimensional demonstration of the microchannel.

The numerical computation was carried out with a numerical grid, as shown in Figure 2, where the white color shows the regions of very dense mesh.

Different grades of grid refinement were tested. The grid refinement research demonstrated that a total number of about 3,399,973 elements was sufficient to acquire a grid-independent solution.

The single-phase model and Lagrangian approach were simulated using the control volume method (FVM).

In numerical tests, the forces such as drag, thermophoretic, and Brownian etc., which arose as a result of the interaction between the base fluid and the nanoparticles, were taken into account under the Lagrangian solution approach. These forces were included in the source term in the momentum equation.

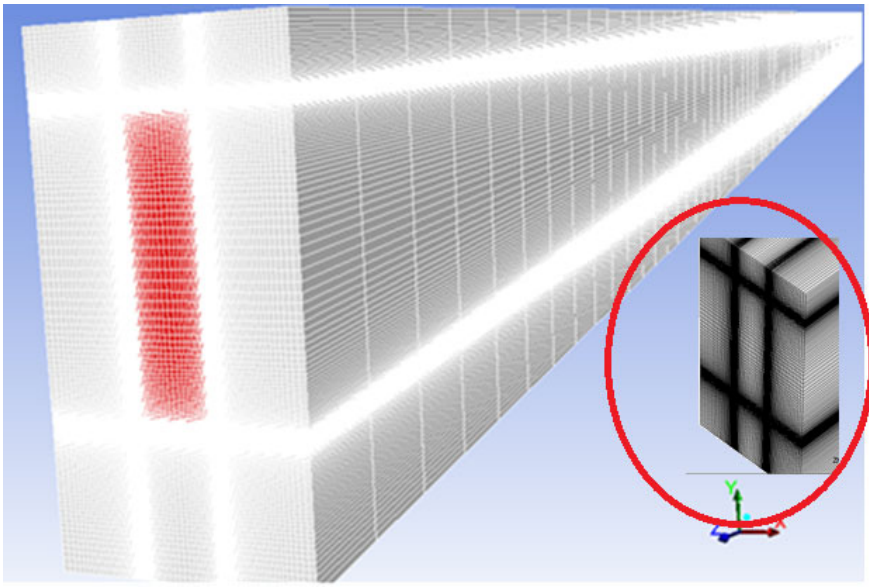

Figure 2. CFD surface mesh for the microchannels.

The SIMPLE algorithm was employed for pressure–velocity coupling. The second order upwind discretization method was adopted to test the stability of solution convergence. The DPM as the two-way coupling method was used to track nanoparticle trajectories. In this study, the convergence criteria for continuity, momentum and energy equations were set to 10^{-6}, 10^{-6} and 10^{-9}, respectively.

2.3. Nanofluid Properties

Some properties of BN, Al_2O_3, TiO_2, CuO and pure water, such as density, specific heat and thermal conductivity at 303.15 K, are given in Table 1.

Table 1. Thermophysical properties of Nanoparticles and Pure Water at 303.15 K.

Property	Water	Al_2O_3	TiO_2	CuO	BN
Density (kg/m^3)	998.2	3970	4050	6500	2300
Specific heat (J/kg.K)	4182	765	697	536	1150
Thermal conductivity (W/m.K)	$-0.93314 + 0.00853 \cdot T - 0.000011259 \cdot T^2$ [17]	25	11.8	20	52
Viscosity (kg/m.s)	$0.01723 - 9.25951e^{-5} \cdot T + 1.2681e^{-7} \cdot T^2$ [17]	-	-	-	-

Some properties of nanofluids such as thermal conductivity (k), dynamic viscosity (μ), specific heat (c) and density (ρ) can be shown with the following equations [31]:

$$k_{nf} = \left[\frac{k_p + (n-1)k_{bf} - (n-1)\phi(k_{bf} - k_p)}{k_p + (n-1)k_{bf} + \phi(k_{bf} - k_p)}\right] k_{bf} \quad (12)$$

$$\frac{\mu_{nf}}{\mu_{bf}} = 1 + 2.5\phi \quad (13)$$

$$c_{nf} = (1-\phi)c_{bf} + \phi c_p \quad (14)$$

$$\rho_{nf} = (1-\phi)\rho_{bf} + \phi\rho_p \quad (15)$$

where nf, bf and p are the properties of the nanofluid, pure water and solid particle, ϕ is the volume fraction rate, and n is the shape factor of the solid particle.

Figure 3 shows specific heat, thermal conductivity, viscosity and density for coolants of Al_2O_3/Water, TiO_2/Water, CuO/Water and BN/water at volume fraction ratio of 3% and of pure water. 3% volume fraction was chosen in the figure because the thermal conductivity, viscosity, density increase as the particle concentration increase, but the specific heat decreased with the increase of particle concentrations.

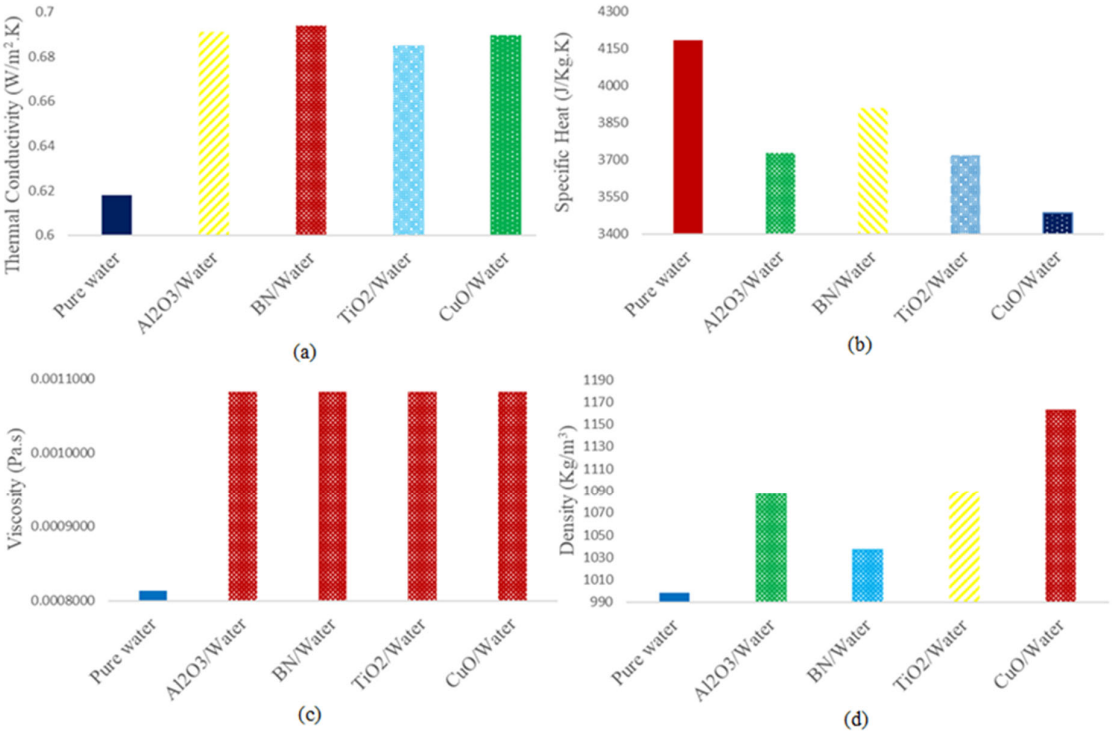

Figure 3. Properties of nanofluids and pure water at volume fraction ratio of 3% and 303.15 K for (**a**) Thermal conductivity, (**b**) Specific heat, (**c**) Viscosity and (**d**) Density.

As can be seen from this figure, the properties of the coolant change in different mixtures. In the transition from base fluid water to nanofluid, thermal conductivity, viscosity and density values increase while specific heat decreases.

3. Results and Discussion

In this paper, to obtain the effect of the use of boron nitride (BN) and other conventional nanoparticles (Al_2O_3, CuO and TiO_2) in a microchannel on pressure drop and heat transfer, the 3-D numerical simulations using fluent CFD code were assessed, as well as the microchannels for different volume fraction of nanofluids. Boron nitride and other conventional nanoparticles (Al_2O_3, CuO and TiO_2) were used with water as a base fluid by changing the inlet Reynolds numbers. An evaluation was carried out to establish which of these four nanoparticles were considered to have superior properties in terms of pressure drop and heat transfer characteristics.

3.1. Numerical Validation

Firstly, the numerical technique was verified with the results given in Shi et al. [17]. The inlet temperature of fluid had a constant value of 303.15 K for different Reynolds numbers. A uniform heat flux, q = 200,000 W/cm^2, was applied to the bottom surface of the microchannel.

Figure 4 shows the comparison of the pressure drop values for different Reynolds numbers with water and water/Al_2O_3 fluids obtained using the numerical tests with the results given in Shi et al. [17].

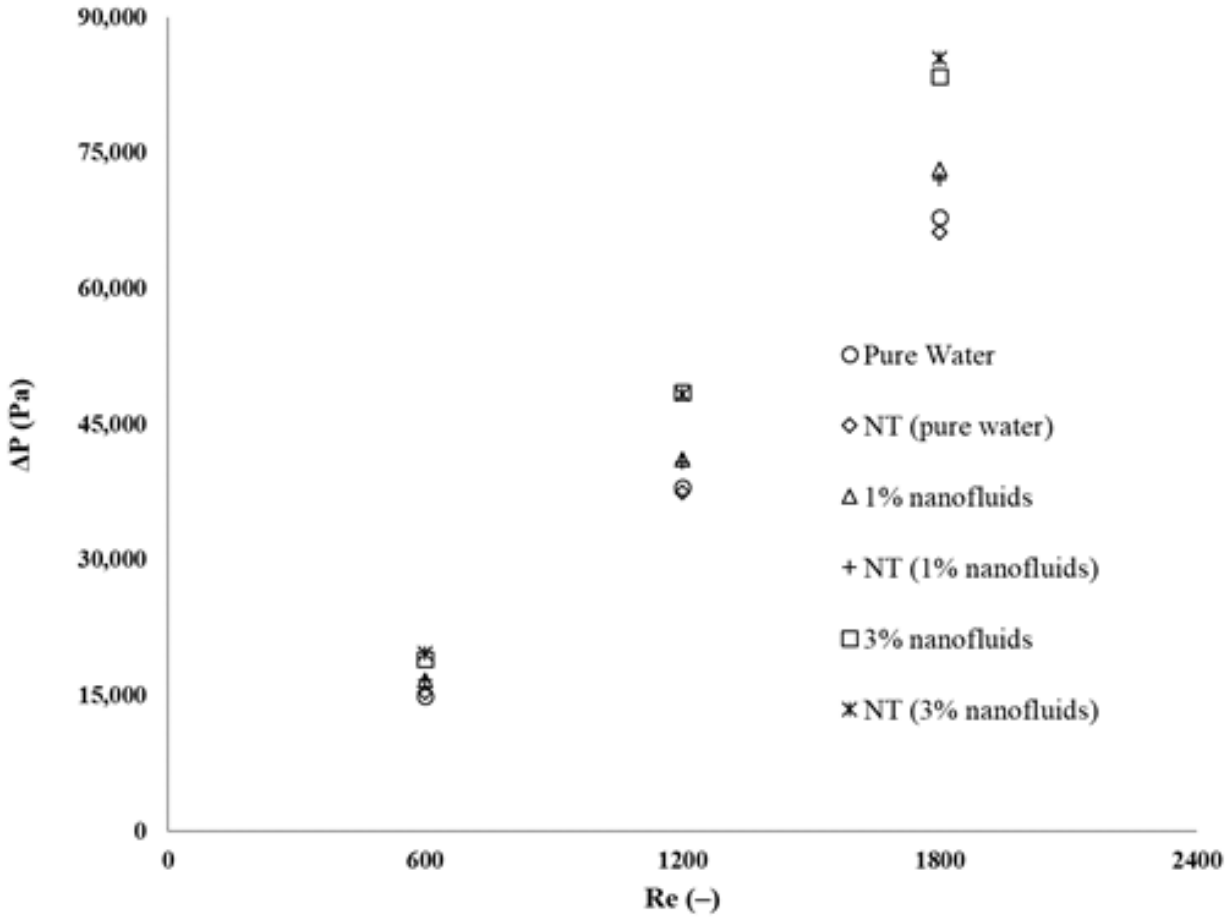

Figure 4. Comparison of the pressure drop values for different Reynolds numbers with water and water/Al_2O_3 fluids obtained by the numerical tests (NT) with the results given in Shi et al. [17].

As can be seen from Figure 4, the pressure drop increases with the increasing Reynolds numbers, so it can be seen clearly that the consumption of pumping power directly increases. Moreover, the pressure drop also increases owing to the increase of the mixture density and viscosity with the addition of 1% and 3% Al_2O_3 as nano-particles. Results obtained from the numerical tests show good agreement with results given in Shi et al. [17].

Figure 5 gives the comparison of the heat transfer coefficients values for different Reynolds numbers with water and water/Al_2O_3 fluids obtained using the numerical tests with the results given in Shi et al. [17].

As can be seen from Figure 5, the heat transfer coefficient increases with the increasing Reynolds number, so it is clear that the thermal performance directly increases. Moreover, the thermal performance also increases due to the improvement of the thermal properties such as the thermal conductivity coefficient with the addition of 1% and 3% Al_2O_3 as nanoparticles. Results obtained using the numerical tests demonstrate good agreement with results given in Shi et al. [17].

After the numerical technique was verified, the maximum temperature differences obtained for different Re and pure water in the microchannel and their contours were obtained in Figures 6 and 7. It can be seen that the maximum temperature decreases with the increasing Reynolds numbers since the thermal resistance decreases as the Reynolds numbers increases. This nonlinear trend is in agreement with already published papers [32]. Figure 8 gives the results of the friction factor values obtained using numerical tests for different Reynolds numbers and pure water.

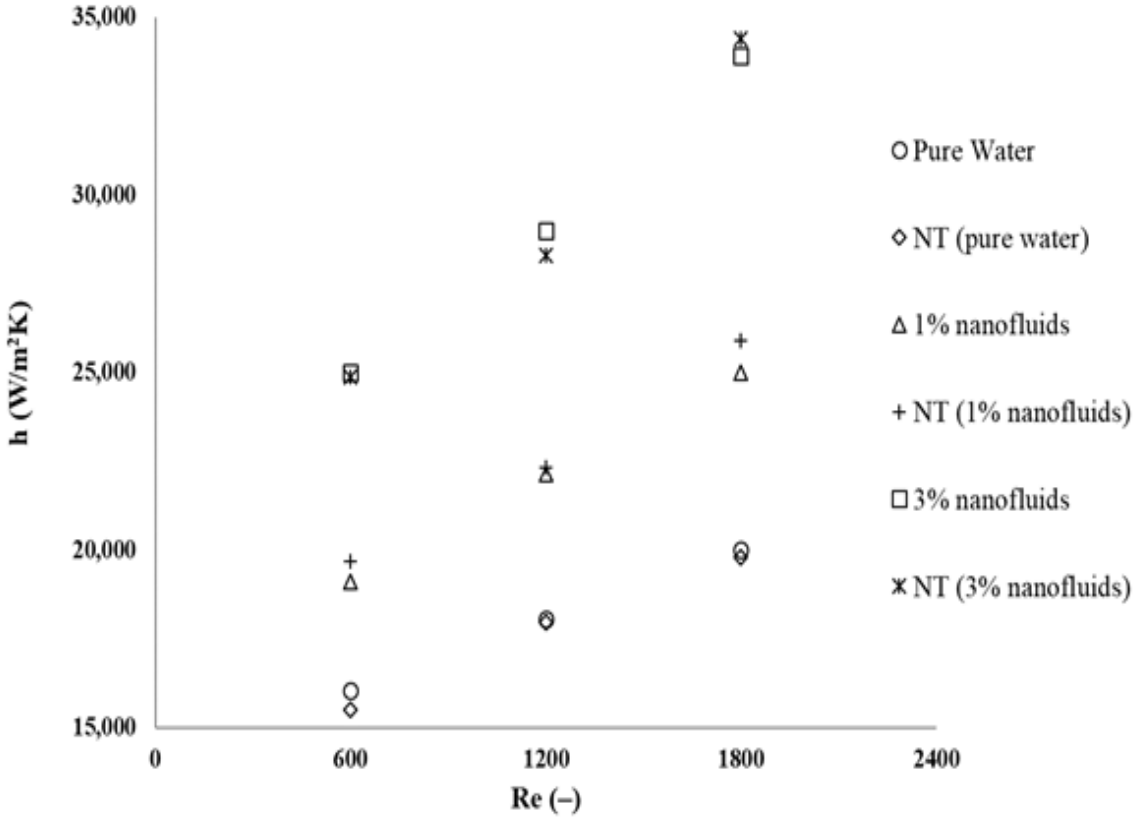

Figure 5. Comparison of the heat transfer coefficients values for different Reynolds numbers with water and water/Al_2O_3 fluids obtained using the numerical tests (NT) with the results given in Shi et al. [17].

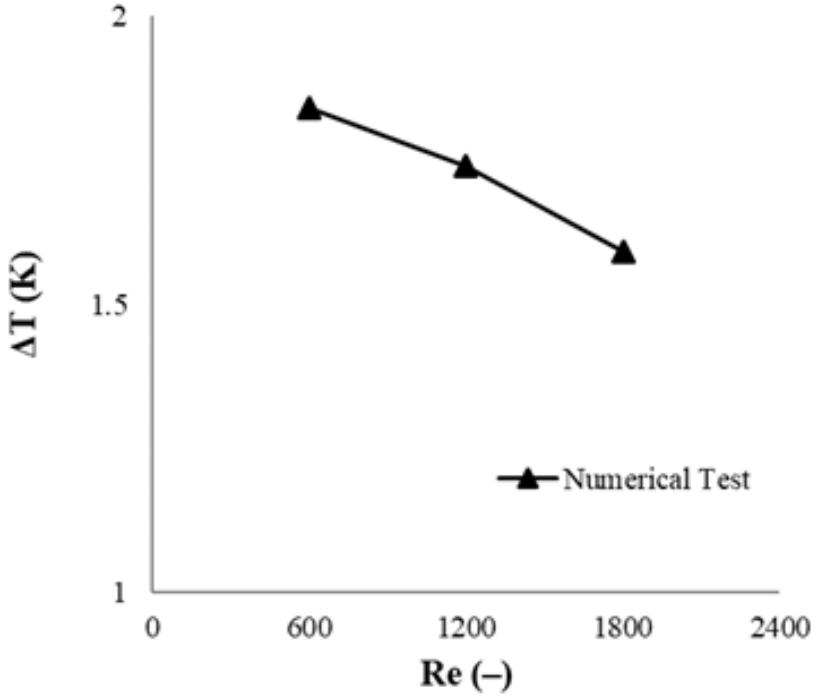

Figure 6. Comparison of maximum temperatures (K) obtained by changing Reynolds numbers (pure water).

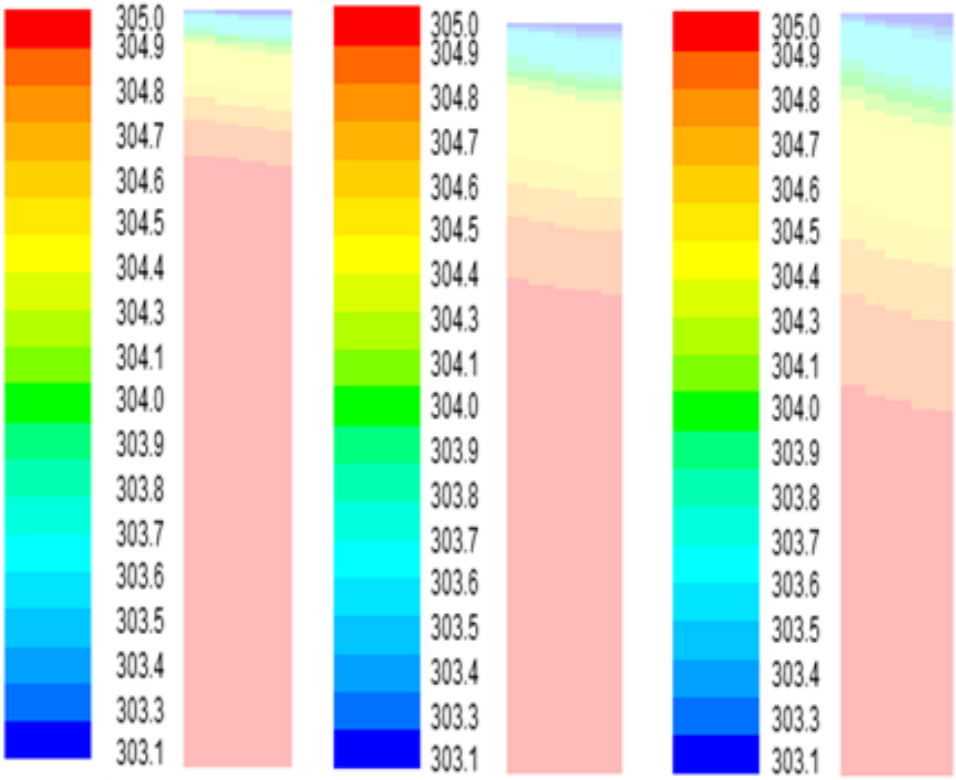

Figure 7. Comparison of the temperature contour (K) obtained numerically for pure water with Re = 600, 1200 and 1800, respectively.

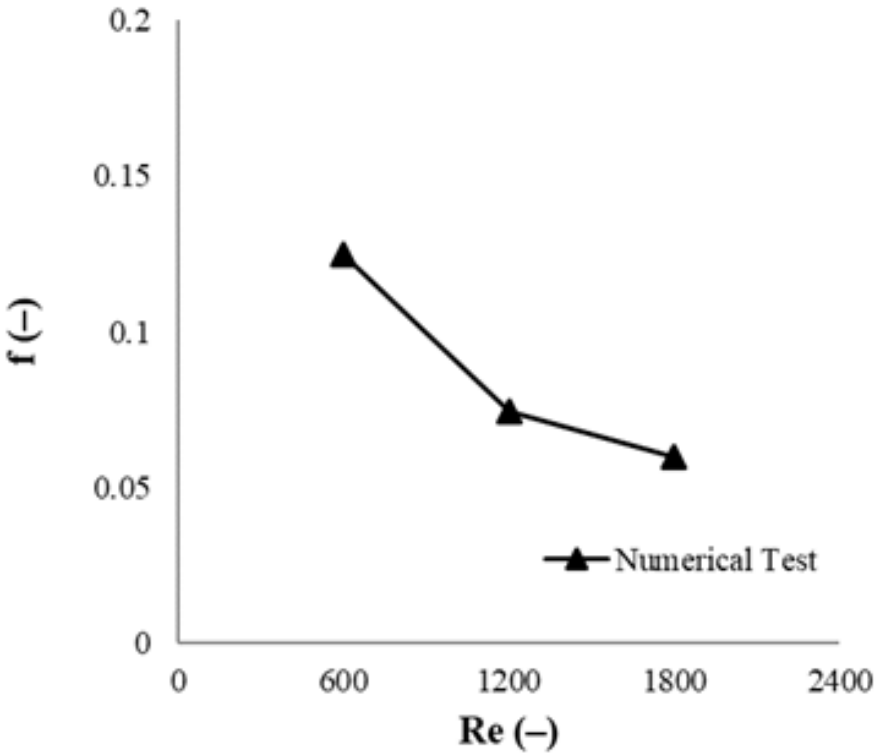

Figure 8. Comparison of friction factor values obtained by changing Reynolds numbers (pure water).

The friction coefficient decreased with the increasing Reynolds numbers, and it was almost constant with high Reynolds numbers (Figure 8). The reason is that at low Reynolds numbers, viscous effects and friction coefficient of the fluid flow are high. Viscous effects

decrease with the increasing Reynolds numbers, therefore decreasing the effects of surface friction. The friction coefficient then finally becomes almost constant.

3.2. Analysis of Performance Characteristics of Nanofluids

The effect of the use of boron nitride and other conventional nanoparticles (Al_2O_3, CuO and TiO_2) in a microchannel on pressure drop and heat transfer were studied in detail.

As can be seen from the above validation results, the heat transfer coefficient and pressure drop increased by adding nanoparticles to pure water. At the same time, when the volume fraction ratio was increased from 1% to 3%, the heat transfer coefficient increased due to the thermal conductivity of the nanofluid increases.

A comparison of the longitudinal development of heat transfer coefficient values along the microchannel for Al_2O_3/Water, TiO_2/Water, CuO/Water and BN/water at a volume fraction of 3%, obtained using numerical tests, is given in Figure 9.

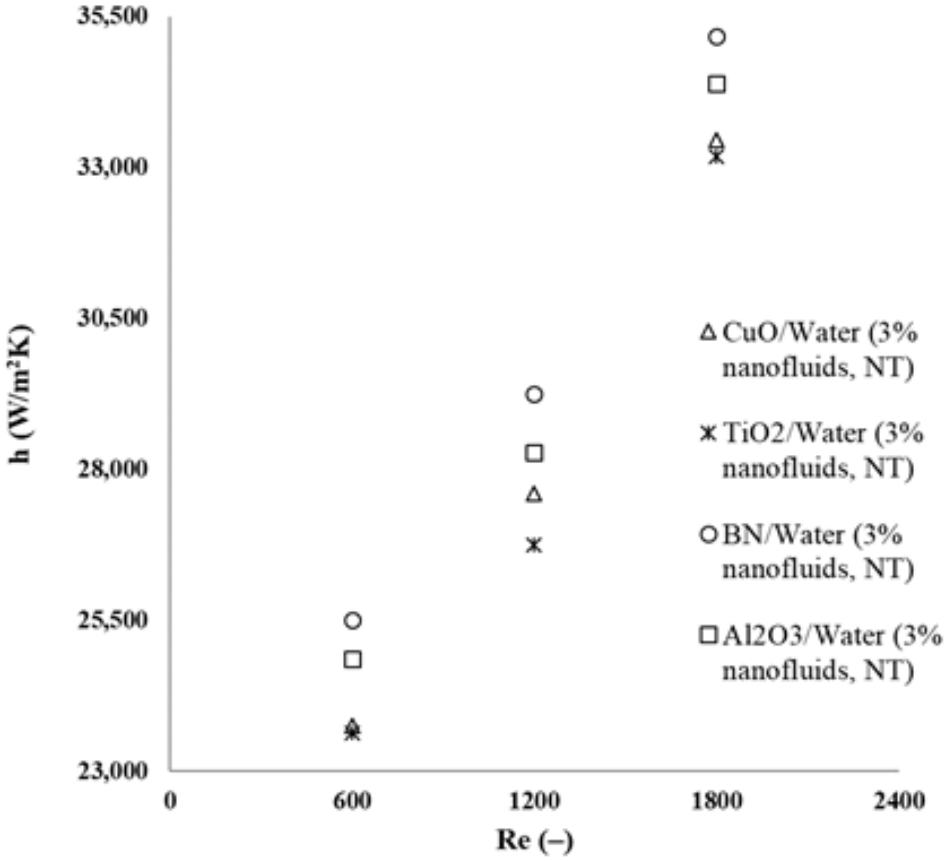

Figure 9. Comparison of the heat transfer coefficients values for different Reynolds numbers obtained using numerical tests (NT).

As can be seen from Figure 9, the heat transfer coefficient of BN is some higher compared with other conventional nanoparticles (Al_2O_3, CuO and TiO_2) for the same Reynolds numbers, because it is clear that BN, when compared with Al_2O_3, CuO and TiO_2 nanoparticles, has high thermal properties.

A comparison of the longitudinal development of pressure drop values along the microchannel for Al_2O_3/Water, TiO_2/Water, CuO/Water and BN/water at the volume fraction = 3%, obtained using numerical tests, is given in Figure 10.

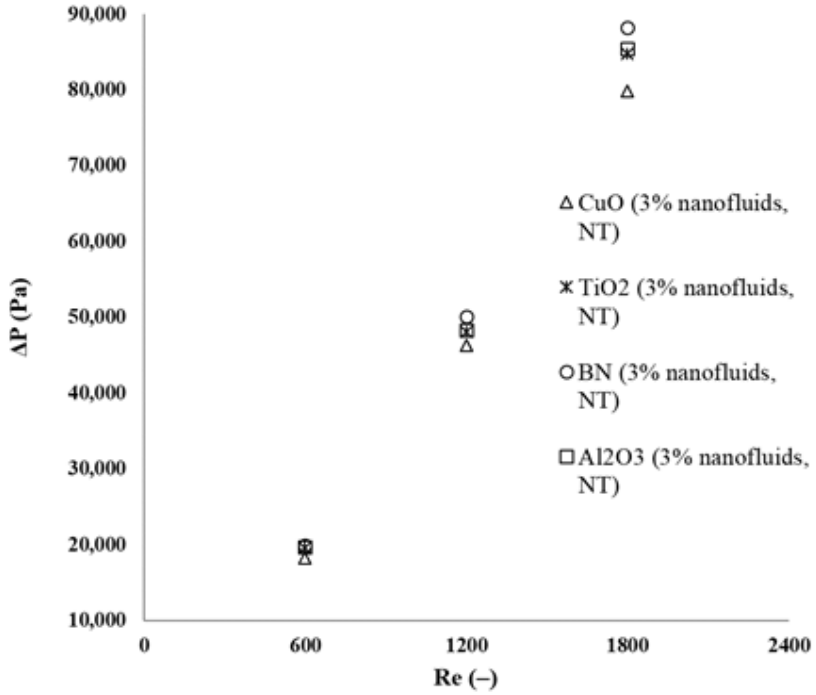

Figure 10. Comparison of the pressure drop values for different Reynolds numbers obtained using numerical tests (NT).

As can be seen from Figure 10, the pressure drop values of BN is slightly higher compared with other nanoparticles for the same Reynolds numbers, as it is clear that BN has the high velocity profiles due to its low density.

In cooling systems, it is desirable for the heat transfer properties to be high, but for the pressure losses to be minimal. The changing of geometric parameters to increase the heat transfer properties and reduce the pressure loss yields no results because the configurations which are made to improve heat transfer lead to too high an increase in pressure loss. In this case, the best thing to do is to add nanoparticles to the fluid to obtain a new fluid called nanofluid. When the relevant literature is taken into account, it is seen that Al_2O_3/water is the most commonly used nanofluid.

In the comparison between BN and the widely used Al_2O_3, considering the heat transfer parameters, it is seen that BN is the more suitable nanoparticle with a very small increase in pressure losses. TiO_2 and CuO, which are also studied in numerical tests, are not suitable compared to BN and Al_2O_3 in terms of heat transfer with very small pressure differences.

4. Conclusions

In this paper, to obtain the effect of the use of boron nitride and other conventional nanoparticles (Al_2O_3, CuO and TiO_2) in a microchannel on pressure drop and heat transfer, the 3-D numerical simulations were assessed using the fluent CFD code of the microchannels. Al_2O_3, TiO_2, CuO and BN nanoparticles were used with water as a base fluid by changing the inlet Reynolds number and the volume fraction ratio. An evaluation was carried out to establish which of these four nanoparticles have superior properties in terms of pressure drop and heat transfer characteristics.

The pressure drop increased with the increasing Reynolds number, so it is clear that the consumption of pumping power directly increases. Moreover, the pressure drop also increased due to the increase of viscosity with the addition of 1% and 3% nanoparticles.

The heat transfer coefficient increased with the increasing Reynolds number, so it is clear that the thermal performance directly increases. Moreover, the thermal performance also increased due to the improvement of the thermal properties with the addition of 1% and 3% nanoparticles.

The maximum temperature decreases with the increasing Reynolds numbers because the thermal resistance decreases as the Reynolds numbers increases.

The properties of the fluid pair significantly affect heat transfer and pressure drop. It can be concluded that the improvement of the heat transfer and pressure drop in the microchannel relates to the properties of fluid pattern.

Compared to other conventional nanoparticles (Al_2O_3, CuO and TiO_2), BN improves heat transfer and slightly increases pressure drop due to its high thermal conductivity and high velocity profile due to low density. It is also chemically stable at the highest temperature relative to most solid materials. Thus, it has a structure that can be used in cooling systems for a long time without causing a problem of agglomeration.

The friction coefficient decreased with the increasing Reynolds numbers, and it was almost constant at high Reynolds numbers. The reason is that at low Reynolds numbers, viscous effects and the friction coefficient of the fluid flow are high. Viscous effects decreased with the increasing Reynolds numbers, therefore decreasing the effects of surface friction. The friction coefficient finally becomes almost constant.

Funding: This research received no external funding.

Institutional Review Board Statement: Not applicable.

Informed Consent Statement: Not applicable.

Data Availability Statement: Not applicable.

Conflicts of Interest: The author has no conflict to disclose.

References

1. Naqiuddin, N.H.; Saw, L.H.; Yew, M.C.; Yusof, F.; Ng, T.C.; Yew, M.K. Overview of micro-channel design for high heat flux application. *Renew. Sustain. Energy Rev.* **2018**, *82*, 901–914. [CrossRef]
2. Zhou, J.; Cao, X.; Zhang, N.; Yuan, Y.; Zhao, X.; Hardy, D. Micro-channel heat sink: A review. *J. Therm. Sci.* **2020**, *29*, 1431–1462. [CrossRef]
3. Kandlikar, S.G.; Grande, W.J. Evolution of Microchannel Flow Passages–Thermohydraulic Performance and Fabrication Technology. *Heat Transf. Eng.* **2003**, *24*, 3–17. [CrossRef]
4. Shao, N.; Gavriilidis, A.; Angeli, P. Flow Regimes for Adiabatic Gas–Liquid Flow in Microchannels. *Chem. Eng. Sci.* **2009**, *64*, 2749–2761. [CrossRef]
5. Bermejo, P.; Revellin, R.; Charnay, R.; Garbrecht, O.; Hugon, J.; Bonjour, J. Modeling of a Microchannel Evaporator for Space Electronics Cooling:Entropy Generation Minimization Approach. *Heat Transf. Eng.* **2013**, *34*, 303–312. [CrossRef]
6. Gong, L.; Zhao, J.; Huang, S. Numerical Study on Layout of Micro-Channel Heat Sink for Thermal Management of Electronic Devices. *Appl. Therm. Eng.* **2015**, *88*, 480–490. [CrossRef]
7. Kaya, F. Numerical Investigation of Effects of Ramification Length and Angle on Pressure Drop and Heat Transfer in a Ramified Microchannel. *J. Appl. Fluid Mech.* **2016**, *9*, 767–772. [CrossRef]
8. Saenen, T.; Baelmans, M. Numerical Model of a Two-Phase Microchannel Heat Sink Electronics Cooling System. *Int. J. Therm. Sci.* **2012**, *59*, 214–223. [CrossRef]
9. Sharma, C.S.; Tiwari, M.K.; Michel, B.; Poulikakos, D. Thermofluidics and Energetics of a Manifold Microchannel Heat Sink for Electronics with Recovered Hot Water as Working fluid. *Int. J. Heat Mass Transf.* **2013**, *58*, 135–151. [CrossRef]
10. Zunaid, M.; Jindal, A.; Gakhar, D.; Sinha, A. Numerical Study of Pressure Drop and Heat Transfer in a Straight Rectangular and Semi Cylindrical Projections Microchannel Heat Sink. *J. Therm. Eng.* **2017**, *3*, 1453–1465. [CrossRef]
11. Prasad, A.R.; Singh, S.; Nagar, H. A Review on Nanofluids: Properties and Applications. *Int. J. Adv. Res. Innov. Ideas Educ.* **2017**, *3*, 3185–3209.
12. Das, S. Nanofluids for Heat Transfer: An Analysis of Thermophysical Properties. *IOSR J. Appl. Phys.* **2015**, *7*, 34–40.
13. Abdollahi, A.; Mohammed, H.A.; Vanaki, S.M.; Osia, A.; Haghighi, M.R.G. Fluid Flow and Heat Transfer of Nanofluids in Microchannel Heat Sink with V-Type Inlet/Outlet Arrangement. *Alex. Eng. J.* **2017**, *56*, 161–170. [CrossRef]
14. Coskun, T.; Cetkin, E. Heat Transfer Enhancement in a Microchannel Heat Sink: Nanofluids and/or Micro Pin Fins. *Heat Transf. Eng.* **2020**, *41*, 1818–1828. [CrossRef]
15. Sabaghan, A.; Edalatpour, M.; Moghadam, M.C.; Roohi, E.; Niazmand, H. Nanofluid Flow and Heat Transfer in a Microchannel with Longitudinal Vortex Generators: Two-Phase Numerical Simulation. *Appl. Therm. Eng.* **2016**, *100*, 179–189. [CrossRef]
16. Belhadj, A.; Bouchenafa, R.; Saim, R. Numerical Investigation of Forced Convection of Nanofluid in Microchannels Heat Sinks. *J. Therm. Eng.* **2018**, *4*, 2263–2273. [CrossRef]
17. Shi, X.; Li, S.; Wei, Y.; Gao, J. Numerical Investigation of Laminar Convective Heat Transfer and Pressure Drop of Water-Based Al_2O_3 Nanofluids in a Microchannel. *Int. Commun. Heat Mass Transf.* **2018**, *90*, 111–120. [CrossRef]

18. Kahani, M. Simulation of Nanofluid Flow Through Rectangular Microchannel by Modified Thermal Dispersion Model. *Heat Transf. Eng.* **2020**, *41*, 377–392. [CrossRef]
19. Gonçalves, I.M.; Rocha, C.; Souza, R.R.; Coutinho, G.; Pereira, J.E.; Moita, A.S.; Moreira, A.L.N.; Lima, R.; Miranda, J.M. Numerical Optimization of a Microchannel Geometry for Nanofluid Flow and Heat Dissipation Assessment. *Appl. Sci.* **2021**, *11*, 2440. [CrossRef]
20. Zainon, S.N.M.; Azmi, W.H.; Hamisa, A.H. Thermo-physical Properties of TiO_2-SiO_2 Hybrid Nanofluids Dispersion with Water/Bio-glycol Mixture. *J. Phys. Conf. Ser.* **2021**, *2000*, 012003. [CrossRef]
21. Saba, F.; Noor, S.; Ahmed, N.; Khan, U.; Mohyud-Din, S.T.; Bano, Z.; Sherif, E.-S.M.; Khan, I. Heat Transfer Enhancement by Coupling of Carbon Nanotubes and SiO_2 Nanofluids: A Numerical Approach. *Processes* **2019**, *7*, 937. [CrossRef]
22. Rashid, U.; Baleanu, D.; Liang, H.; Abbas, M.; Iqbal, A.; ul Rahman, J. Marangoni Boundary Layer Flow and Heat Transfer of Graphene–Water Nanofluid with Particle Shape Effects. *Processes* **2020**, *8*, 1120. [CrossRef]
23. Han, W.; Wang, L.; Zhang, R.; Ge, C.; Ma, Z.; Yang, Y.; Zhang, X. Water-Dispersible Boron Nitride Nanospheres with High Thermal Conductivity for Heat-Transfer Nanofluids. *Eur. J. Inorg. Chem.* **2017**, *46*, 5466–5474. [CrossRef]
24. Hou, X.; Wang, M.; Fu, L.; Chen, Y.; Jiang, N.; Lin, C.T.; Wang, Z.; Yu, Z. Boron Nitride Nanosheet Nanofluids for Enhanced Thermal Conductivity. *Nanoscale* **2018**, *10*, 13004–13010. [CrossRef]
25. Velmurugan, V.; Bharathithasan, I.; Grace, A.N. Synthesis and Physiothermal Analysis of Boron Nitride Based Nanofluid. *Indian J. Sci. Technol.* **2016**, *9*, 39. [CrossRef]
26. Kumar, S.; Tiwari, A.K. Performance evaluation of evacuated tube solar collector using boron nitride nanofluid. *Sustain. Energy Technol. Assess.* **2022**, *53*, 102466. [CrossRef]
27. Zhu, J.; Li, X.; Yang, R.; Wen, J.; Li, X. Photothermal conversion characteristics and exergy analysis of TiN@h-BN composite nanofluids. *J. Mater. Sci.* **2022**, *57*, 19799–19816. [CrossRef]
28. Mat, M.N.H.; Mohd-Ghazali, N.; Shamsuddin, H.S.; Estellé, P. Thermofuid behaviour of boron nitride nanotube nanofuid in a microchannel under optimized conditions. *J. Therm. Anal. Calorim.* **2022**. [CrossRef]
29. Kleinstreuer, C.; Xu, Z. Mathematical Modeling and Computer Simulations of Nanofluid Flow with Applications to Cooling and Lubrication. *Fluids* **2016**, *1*, 16. [CrossRef]
30. Bianco, V.; Chiacchio, F.; Manca, O.; Nardini, S. Numerical investigation of nanofluids forced convection in circular tubes. *Appl. Therm. Eng.* **2009**, *29*, 3632–3642. [CrossRef]
31. Lee, J.; Mudawar, I. Assessment of the effectiveness of nanofluids for single-phase and two-phase heat transfer in micro-channels. *Int. Jounal Heat Mass Transf.* **2007**, *50*, 452–463. [CrossRef]
32. Bello, O.T.; Meyer, J.P.; Ighalo, F.U. Combined Numerical Optimization and Constructal Theory for the Design of Microchannel Heat Sinks. *Numer. Heat Transf. A* **2010**, *58*, 882–899. [CrossRef]